Catalysis Today 151 (2010) 347–353

Contents lists available at ScienceDirect

Catalysis Today

journal homepage: www.elsevier.com/locate/cattod

Effects of different regeneration timing protocols on the performance of a model NO_X storage/reduction catalyst

Meshari AL-Harbi, William S. Epling *

Department of Chemical Engineering, University of Waterloo, 200 University Ave W, Waterloo, ON, N2L 3G1 Canada

ARTICLE INFO

Article history:
Available online 8 January 2010

Keywords:
NO_X storage
NO_X regeneration
NO_X reduction
Vehicle emission

ABSTRACT

The effects of different regeneration times, but with a constant total amount of reductant delivered, were investigated over a model NO_X storage and reduction (NSR) catalyst. The different regeneration times were 4, 8 and 16 s with 4, 2, and 1% H_2 as the reductant amounts, respectively. The lean time was kept the same during these experiments, resulting in a constant inlet NO_X-to-reductant amount in the cycles. Overall, the results show clear improvements with longer regeneration times in both NO_X trapping and overall reduction performance at all temperatures except 500 °C. At 500 °C, there was still an increase in trapping performance with longer regeneration time, but a more significant increased NO_X release coincident with a small increase in the trapping performance resulted in an overall decrease in NO_X conversion with increasing regeneration time. The data demonstrate that the different concentrations of H_2 did not lead to different regeneration extents, but that the main factor for the improved performance was the regeneration time itself. With longer regeneration times, more nitrate/nitrite decomposition occurred, thereby leading to more extensive surface cleaning.

1. Introduction

With growing concern and public awareness about the environmental, ecological and health impacts of air pollution and global warming, environmental agencies have been setting increasingly stringent regulations to mitigate and control vehicle emissions. This is made more difficult by a coincident demand for higher fuel economy. One solution is a shift from stoichiometric burn engines, such as today's standard gasoline engine, to lean-burn gasoline or diesel engines. Such a transition could result in a reduction in both fuel consumption and CO_2 emissions. A significant challenge that still remains is NO_X emissions. NO_X storage and reduction (NSR) catalysis is one of the currently accepted and implemented technologies for lean-burn engine NO_X emissions control. NSR catalysts are typically composed of precious metals such as Pt, Pd, and Rh for the redox reactions, and alkali and alkaline metal earth components that trap NO_X in the form of nitrites and nitrates, all supported on a high surface area substrate such as γ-alumina [1–4]. This technology cycles through two phases; a lean and a rich phase. In the lean phase NO is oxidized to NO_2 on the precious metal sites and then NO_2 is adsorbed by the trapping materials, such as Ba in the form of $Ba(NO_3)_2$ and/or $Ba(NO_2)_2$ [5–7]. In operation, the lean phase continues until some level of NO_X slips past the catalyst. At this stage, the rich phase of the cycle is started, where reductants such as CO, H_2, and hydrocarbons are introduced to reduce the surface NO_X species to N_2, thereby regenerating the trapping sites for the next lean phase, with reduction occurring also via participation of the precious metals sites [8–10].

Numerous studies have investigated regeneration phenomena, including the effect of reductant type, reductant amount, and different lean and rich times [10–16]. In terms of reductant type [11], the reduction efficiencies of H_2, CO, C_3H_6 and C_3H_8 at different temperatures were investigated over a $Pt/BaO/Al_2O_3$ model catalyst. The results showed that H_2 was a superior reductant at low temperatures ($T \leq 250$ °C), while at high temperatures H_2 and CO were similar and showed higher reduction efficiency than C_3H_6. C_3H_8 was inefficient at all temperatures tested. Similar observations were also reported over a commercial NSR catalyst [10]. The effect of H_2 and CO amounts on the overall performance of a commercial NSR catalyst was also investigated [14]. The performance of the catalyst improved with each incremental increase in H_2 concentration, with 5% H_2 the highest level evaluated. At high temperature, the performance also increased with increasing CO amounts, however at 200 °C, increasing CO was found to decrease performance due to precious metal site poisoning.

The effect of the lean and rich times on the performance of a model NSR catalyst was also investigated, using H_2, CO, and C_3H_6 as reducing agents [15]. As an example of the results, at 300 °C, when the lean time was increased from 45 to 135 s while

---

* Corresponding author.
E-mail address: wepling@cape.uwaterloo.ca (W.S. Epling).

0920-5861/$ – see front matter © 2009 Elsevier B.V. All rights reserved.
doi:10.1016/j.cattod.2009.12.004

maintaining a constant rich time (1.5 s), the overall conversion decreased from 93 to 40%. This was attributed to a lack of sufficient reductant during the 1.5 s rich phase as the lean time was increased. In the same study, the rich time was increased from 1.5 to 4.5 s with a constant reductant concentration (3%) and lean phase time (135 s), and the NO_X conversion increased from 41 to 98%. This was due to the Ba sites being more extensively regenerated with the longer regeneration time and therefore able to participate in trapping during the following lean phase. At lower operating temperatures ($T \leq 250\,^{\circ}C$), the authors found that NO_X conversion was less dependent on the lean/rich ratio. In another study, the effect of rich time vs. reductant amount on the overall NO_X conversion performance of a powder $Pt/Ba/Al_2O_3$ catalyst was investigated [16]. With a fixed reductant-to-inlet NO_X ratio at 400 °C, the authors concluded that using longer regeneration times with lower reductant concentrations was more efficient compared to short regeneration times with higher reductant concentrations, which they attributed to two effects. The first was consumption of reductant by the oxygen at the lean/rich interface and the second was that the reduction process with the shorter regeneration time was not as efficient as that with longer regeneration.

The overall reduction of NO_X and regeneration of trapping sites during the rich phase depends not only on the amount and type of reductant, but also on the amount of NO_X released via decomposition of the surface nitrite and nitrate species. Primary causes of nitrate/nitrite decomposition and NO_X release are changes is the gas phase composition, such as the absence of oxygen and NO and the presence of CO_2, H_2O and reductant during the rich phase, as well as heat generated from the exothermic reaction between reductants and oxygen stored on the catalyst surface. For the latter, in a previous study [17] the temperature patterns during cyclic operation of a commercial NSR catalyst were investigated. Just after the onset of the rich phase, the measured temperature rise observed within the first few millimeters of the catalyst surpassed 30 °C. As the nitrite/nitrate species stability is a decreasing function of temperature, the increased temperature can lead to decomposition. Such large temperature rises are not typically observed over model $Pt/Ba/Al_2O_3$ samples due to a lack of significant oxygen stored on the surface, and therefore this exotherm driven decomposition would be insignificant on these model systems.

Nova et al. [18] clearly demonstrated the relative unimportance of a purely thermally driven decomposition versus reductant-induced decomposition on a model $Pt/Ba/Al_2O_3$ system. In their study little NO_X desorption/nitrate decomposition was observed during temperature-programmed desorption experiments up to the temperature where NO_X adsorption was performed. However, in the presence of H_2, decomposition could begin at temperatures 200 °C lower than the adsorption temperature. Beyond the reductants, other gas-phase constituents influence nitrate stability as well. The presence of oxygen increases nitrate stability [19] and in its absence, the nitrates/nitrites become less stable and decompose. Similarly, it has been shown that CO_2 and H_2O can influence the stability of surface nitrate species, with CO_2 negatively impacting performance [20] via a reduction in nitrates formed, while H_2O has been observed to both decrease [21] and increase [5] NO_X conversion performance. The effect of Pt on the thermal stability of nitrate and/or nitrite species has also been addressed [22–24,18]. Results show that Pt induces decomposition of the Ba nitrite/nitrate during the regeneration phase and therefore NO_X trapped close to Pt might be released faster. Along the same concept, two types of Ba nitrate have been observed; surface and bulk [25,26]. Previous studies have concluded that surface Ba nitrate species are not as thermally stable as a bulk nitrate species.

In this study, the effect of regeneration time, while keeping the total amount of reductant introduced during the regeneration phase the same, was investigated. The analysis includes experiments with and without reductant to monitor time dependent surface NO_X species decomposition and reductant-induced decomposition. The trapping performance, NO_X release and formation of NH_3 were measured.

2. Experimental methods

The model $Pt/BaO/Al_2O_3$ sample used in this study was supplied by Johnson Matthey in monolithic form. The sample contains 0.12 g/cm^3 Al_2O_3, 1.45% Pt and 20% BaO relative to the Al_2O_3. The sample was cut to 2.1 cm diameter with a length of 6.4 cm from a monolith block that had a cell density of 300 cpsi. The sample was inserted into a horizontal quartz tube, which was placed inside a Lindberg Minimite temperature-controlled furnace. The catalyst was wrapped with 3M insulation material to seal the catalyst in the quartz tube, to ensure that no gas slipped around the sample. For temperature measurements, two *K*-type thermocouples were placed at the radial center of the catalyst; one just inside the inlet face of the catalyst and one just inside the outlet face of the catalyst. A third was placed ~2.5 cm upstream of the sample.

The gases and gas mixtures were supplied by Praxair and were metered with Bronkhorst mass flow controllers. A four-way, fast-acting solenoid valve was used to switch between the lean and rich mixtures, which were made in separate manifolds. After the dry gas mixture had been heated to >120 °C, water was introduced downstream of this valve. Table 1 lists the gas compositions used in the cycling experiments. Small quartz tubes were inserted into the main quartz reactor tube to provide better heat transfer to the gas, such that at the catalyst position, temperature gradients were minimized along the length of catalyst.

Before each experiment, the sample temperature was ramped to 500 °C with 5% H_2O, 5% CO_2, and a balance of N_2 and then the catalyst was cleaned with a gas mixture consisting of 5% H_2O, 5% CO_2, 1% H_2, and a balance of N_2 for 15 min at 500 °C. The reactor was then cooled to the target test temperature. Experiments were performed at 200, 300, 400 and 500 °C with a space velocity, at standard conditions, of 25,000 h^{-1}. Different lean times were used at the different temperatures to reflect the different efficiencies at those temperatures. For example performance at 200 °C is worse than at 300 °C, so longer lean times were used at 300 °C, which also matches application trends better. The gases exiting the reactor were maintained at >190 °C to avoid condensation and NH_3 hold-up. The gas compositions were measured using a MKS MultiGas 2030 FT-IR analyzer at approximately a 2 Hz collection rate. CO, CO_2, NO, NO_2, N_2O, NH_3, and H_2O concentrations were measured.

Table 1
Details of flow conditions used in the experiments.

Flow conditions	Trapping (lean) phase	Regeneration (rich) phase
Space velocity	25,000 h^{-1}	25,000 h^{-1}
Concentrations		
NO	330 ppm	0
O_2	10%	0
CO_2	5%	5%
H_2O	5%	5%
H_2	0	1–4%
N_2	Balance	Balance
Temperature (°C)		
200	40 s	4, 8, 16 s
300	80 s	4, 8, 16 s
400	120 s	4, 8, 16 s
500	80 s	4, 8, 16 s

Table 2
Calculated performance characteristics as a function of temperature, amount of H_2, and regeneration time.

Temperature (°C)	H_2 (%)	Time (s)		NO_X conversion (%)	NO_X trapped (μmol)	NO_X released (μmol)	NH_3 released (μmol)
		Rich	Lean				
200	4	4	40	42	44	4.9	23
	2	8	40	49	51	5.5	28
	1	16	40	57	60	6.4	31
300	4	4	80	79	150	2.8	51
	2	8	80	86	163	3.6	89
	1	16	80	92	175	4.4	99
400	4	4	120	78	226	10	37
	2	8	120	80	237	16	38
	1	16	120	80	247	25	35
500	4	4	80	37	84	15	19
	2	8	80	35	88	23	15
	1	16	80	30	91	34	10

3. Results and discussion

In the first set of experiments, 4, 8 and 16 s regeneration times were used, with 4, 2, and 1% H_2 as the reductant amounts, respectively. Thus the same amount of reductant was introduced during each experiment. As previously shown [14], at low temperature CO as a reductant has a severe negative impact on NSR catalyst performance relative to H_2. However, the same study also demonstrated that if H_2 is added to the reductant stream, some performance can be maintained, and more H_2 led to better performance and less CO poisoning. So although CO was not added to the regeneration mixture in this study, the trends observed with H_2 will still be viable if H_2 is present in any amount in the regeneration gas mixture. The lean phase times at each temperature were maintained during these experiments, resulting in a constant inlet NO_X-to-reductant amount in the cycles. However, different lean times were used at the different temperatures to avoid saturation and 0 ppm NO_X slip at the performance extremes, better reflecting times and saturation levels used in practice. The performance of the catalyst was evaluated at different test temperatures, as listed in Table 2.

The outlet NO_X (the sum of NO + NO_2) concentrations as a function of time obtained during one of the cycles at an inlet temperature of 200 °C are shown in Fig. 1. The lean, or trapping, time was 40 s. The conversions and amounts of NO_X trapped and the amount of unreduced, released NO_X during the rich phase, are listed in Table 2. The amount of unreduced NO_X release is obtained by integrating the quantity of NO_X released during the rich phase, which is defined by the trigger sent to switch the valve controlling which gas phase enters the reactor. All reported values and plotted data were obtained after steady cycle-to-cycle performance was attained. The data plotted in Fig. 1 show that the trapping performance was similar during the first few seconds of the lean phase, no matter the regeneration time, but differed after. The amounts of NO_X trapped were 60, 51, and 44 μmol for the 16, 8, and 4 s regeneration times, respectively. The amounts released as unreduced NO or NO_2 during the rich period were relatively small, but steadily increased as the regeneration time increased. This increase was expected since the amount of NO_X released is a function of NO_X trapped during the previous lean phase, and the amount of NO_X trapped was larger with increasing regeneration time. The total inlet NO_X during the 40 s lean time was 93 μmol. During the regeneration period, with 1, 2, and 4% H_2, 1124 μmol of H_2 were introduced. If the reduction reaction is assumed to be $Ba(NO_3)_2 + 5H_2 \rightarrow N_2 + BaO + 5H_2O$, then for 2 mol of NO_X trapped, 5 mol of H_2 are required for reduction to N_2, or 232 μmol to reduce all the entering NO_X. The catalyst used in these experiments does not contain any oxygen storage components, such as ceria, so the amount of H_2 input was in large excess even if including that needed to consume the very small amount of oxygen stored on the catalyst surface (i.e. Pt oxides and possibly Ba peroxides at low temperatures).

Similar experiments were carried out at 300, 400, and 500 °C to investigate the effect of operating temperature on the storage, release, and reduction of NO_X with the different regeneration protocols. The outlet NO_X concentrations as a function of time at 300 °C are shown in Fig. 2. A summary of the results is also listed in

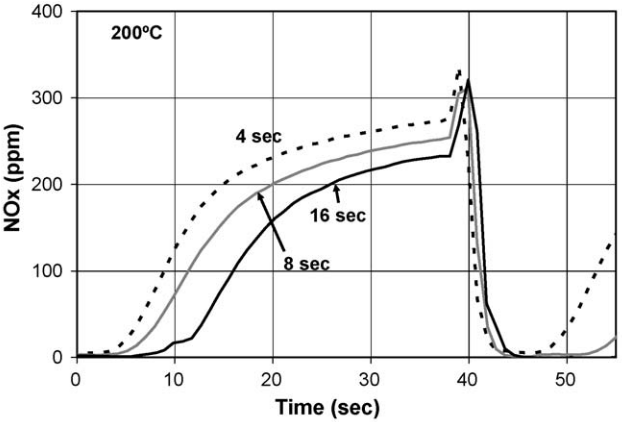

Fig. 1. NO_X outlet concentrations obtained at 200 °C with 1% H_2 and 16 s, 2% H_2 and 8 s, and 4% H_2 and 16 s regeneration phases.

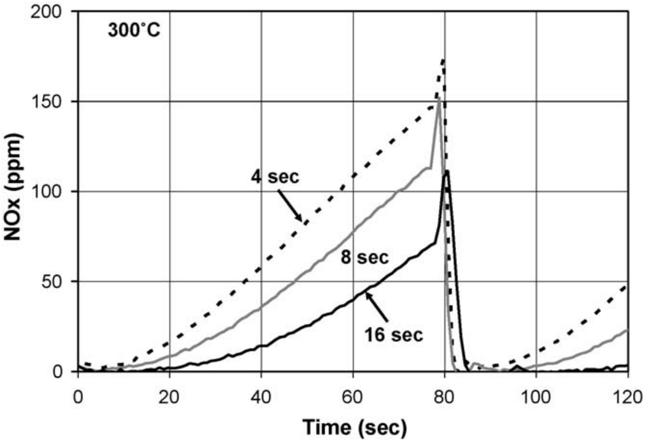

Fig. 2. NO_X outlet concentrations obtained at 300 °C with 1% H_2 and 16 s, 2% H_2 and 8 s, and 4% H_2 and 16 s regeneration phases.

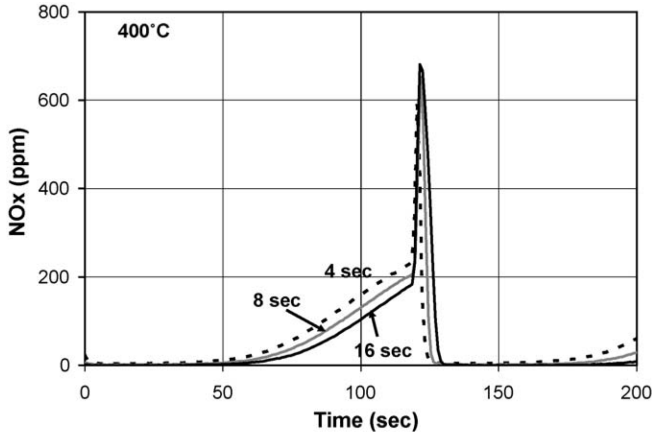

Fig. 3. NO_X outlet concentrations obtained at 400 °C with 1% H_2 and 16 s, 2% H_2 and 8 s, and 4% H_2 and 16 s regeneration phases.

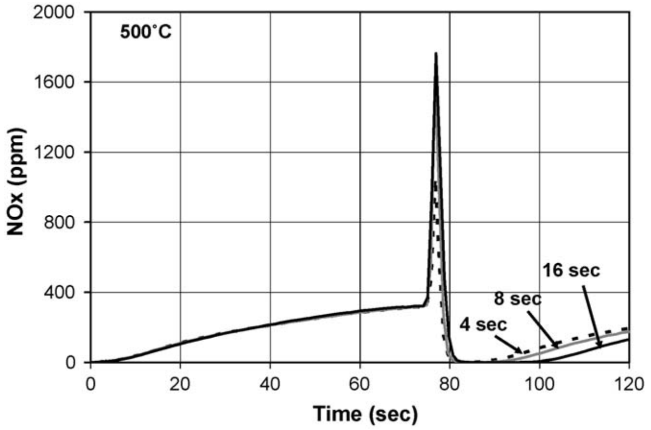

Fig. 4. NO_X outlet concentrations obtained at 500 °C with 1% H_2 and 16 s, 2% H_2 and 8 s, and 4% H_2 and 16 s regeneration phases.

Table 2. Again, there was initially little difference in the performance of the catalyst at the beginning of the lean phase with differences appearing as the lean time progressed. The trapping trends were similar to those observed at 200 °C, where increased regeneration time led to increased amounts trapped. This increase in the amount trapped, with little impact on the amount released, led to higher overall conversions. The total inlet NO_X during the 80 s lean phase was 186 μmol and the amount of H_2 required to reduce this NO_X, if all was trapped, is 464 μmol. The inlet H_2 during regeneration was 1120 μmol, still in significant excess.

Fig. 3 compares the outlet NO_X concentrations at 400 °C, with a lean phase duration of 120 s. At this temperature, the performances for all three regeneration times were similar for a larger portion of the lean phase, relative to that observed at the lower temperatures. Differences were still observed, just much later, and again trapping performance was improved with increasing regeneration time. The observed NO_X release was higher than that observed during the 200 and 300 °C tests, but this increase had little impact on the overall NO_X conversions. The improved trapping performance at 400 °C relative to 200 and 300 °C is related to two main factors. First, at low operating temperature, NO oxidation is kinetically limited [5,27] and most NSR catalyst types attain their maximum oxidation activity between 300 and 400 °C. This would therefore result in higher NO_2 amounts and subsequently more rapid and extensive trapping of NO_X as NO_2 is preferred relative to NO for trapping and nitrate formation [28]. Second, not only does the oxidation activity increase as the temperature increases, but also the extent of regeneration increases. As mentioned, with increasing temperature, nitrates become less stable and in the absence of O_2 and NO_X in the gas stream, a more significant amount decomposes at 400 °C relative to the lower temperatures. Furthermore, at high operating temperature, activation of reductants is not an issue [5], and hence the reductant can easily reduce decomposing nitrate species to N_2. With more extensive regeneration, there is more trapping site availability expected in the subsequent lean phase portion of the cycle.

The data obtained at 500 °C and an 80-s lean phase are shown in Fig. 4. Again, improved trapping was observed with longer regeneration times coincident with increased release during the regeneration phase. At this high temperature, however, the NO_X release increased significantly with each increase in regeneration time; 15, 23, and 34 μmol with 4, 8, and 16 s of regeneration time, respectively. This increase in NO_X release coincident with the relatively smaller increase in the trapping performance with longer regeneration times resulted in an overall decrease in NO_X conversion as the regeneration time was increased. Although the reduction rate increases with temperature, the too rapid decomposition rate of the Ba nitrate species combined with decreasing reductant concentration and its rapid consumption at the onset of the regeneration phase led to the increased significance of released and unconverted NO_X. In further detail, at the beginning of the trapping phase, NO_X is trapped at sites located at upstream positions. These sites become saturated with time and then stop taking part in the trapping process, so downstream sites begin to participate. If the trapping phase is long enough, both upstream and downstream trapping sites will have participated in NO_X trapping. At 500 °C, nitrate decomposition is rapid and upon switching to the rich phase, the reductant interacts with NO_X species trapped at the upstream sites to reduce NO_X and regenerate the surface. The evolved NO_X species originating from the downstream trapping sites move through the catalyst without being reduced, as the reductant is being used to regenerate the upstream sites. This would in turn lead to the observed lower conversion of trapped NO_X to N_2. The amount released was higher with longer regeneration times at 500 °C due to the lower local concentration of reductant throughout the catalyst at the onset of the rich phase, with the reduction reaction therefore more reductant limited during the rapid nitrate decomposition and NO_X release. However, the amount trapped was still higher with longer regeneration time. At the lower test temperatures, the increased NO_X release is at least partially due to the increase in the amount trapped, combined with lesser local reductant concentrations when nitrate decomposition begins as well.

The results show a marked increase in the trapping performance coincident with slight increases in NO_X release and therefore overall performance improvement at all temperatures, except 500 °C, with longer regeneration times even though the delivered reductant amounts were identical. The improvement in catalyst performance when using longer regeneration times can be primarily attributed to two effects. First, there will be an impact from gas mixing at the lean-to-rich transition interface, which will briefly lead to some reductant consumption. As mentioned in Section 1, a previous study [16] investigated the effect of a longer regeneration pulse with a lower concentration of reductant vs. a shorter regeneration pulse with a higher concentration of reductant. The authors found that a better regeneration of the catalyst was achieved with the longer regeneration pulse and lower reductant concentration. One explanation proposed was the consumption of reductants via combustion with oxygen at the interface between the lean and rich phase. With higher reductant concentrations, and the high level of O_2 used in the lean phases, more reductant can be lost compared to the lower reductant concentration case. Therefore, if indeed a significant amount of reductant was consumed at the interface when high concentrations (and a shorter rich pulse) were used in their study, the total amount of reductants delivered to the catalyst beyond the very upstream portion (where the oxidation will occur) will be lower than that when longer regenerations where less reductant concentration was used. Thus, a better regeneration could be expected with longer regeneration. If this mixing effect is significant, then in these experiments, as the rich time increased from 4 to 8 s and 8 to 16 s with decreasing reductant concentrations, the effect should have become less. But the difference between the 8 s, 2% H_2 experiment and the 16 s, 1% H_2 experiment was more significant than the difference between the 4 s, 4% H_2 experiment and the 8 s, 2% H_2 experiment. This indicates that this mixing impact on the observed trends is likely minimal, and there must at least be another factor. Furthermore, the temperature rises were relatively small, on the order of 2–6 °C, and the temperature rise at the front of the catalyst was slightly higher during the shorter regeneration time experiments, relative to the longer regeneration times, in our study, indicating a higher combustion rate. This exotherm impact should, if a significant effect, have led to better regeneration with higher reductant concentrations, which was not observed.

The second effect is related specifically to the regeneration time and nitrate decomposition rate. The two reactions shown below, decomposition of the nitrate species, as well as reduction of the nitrate species, describe in an overall sense what occurs during the regeneration phase.

$$Ba(NO_3)_2 \rightarrow BaO + 2NO + 1.5O_2 \qquad (1)$$

$$Ba(NO_3)_2 + 5H_2 \rightarrow N_2 + BaO + 5H_2O \qquad (2)$$

Nitrate decomposition and NO_X release, reaction (1), depend on several factors including temperature, the presence or absence of O_2, H_2O, CO_2 and NO_X, and the inclusion of oxygen storage components such as Ce in the catalyst washcoat. There was little temperature rise during the rich phase of individual experiments, indicating little effect of changing temperature on NO_X release, although this effect might play a more significant role in commercial catalysts [17]. Reaction (1) is the reverse of the trapping reaction, and the absence of oxygen during the regeneration phase can drive the decomposition of Ba nitrate as shown. An oxygen source is required for stabilization and formation of Ba nitrate and if oxygen is not introduced during the regeneration event, the decomposition reaction will be favored. The presence of CO_2 and H_2O coincident with the absence of oxygen during regeneration event also induces the decomposition of Ba nitrate [29–33]. However, in each of these experiments, the inlet CO_2, H_2O and O_2 conditions were identical and therefore should not directly cause the observed changes in performance.

To clarify the effect of the rich phase duration, a second set of cycling experiments at 200 °C was performed, where the most significant difference in overall performance was observed. The cycling experiments were identical to the previous experiments, but in the last cycle after steady cycle-to-cycle performance reached, the reductant was not included during the regeneration phase. The NO_X concentration data as a function of time for these experiments are not plotted, but the outlet NO_X ppm data from each experiment were identical for each incremental time frame. During this phase, the amounts of NO_X trapped in the previous part of the cycle and that released without reductant present are shown in Table 3. The differences between the amount trapped with reductant used in the previous rich phase, and the amount released in the absence of H_2 in the regeneration phase are also listed. The amount of NO_X released in the absence of reductant of course increased as the regeneration time increased. The difference represents the amount of NO_X associated with trapping sites being regenerated during a rich phase when reductant is present, since steady cycle-to-cycle performance had been obtained. The values are quite similar with the three different regeneration times, indicating a similarity in the amount of regenerated trapping sites between the three experiments with three different regeneration times. This indicates that, in terms of a reductant dependency, the amount regenerated is a function of total reductant delivered, and not the concentration. Furthermore, this indicates that the reduction process was not simply slower with short regeneration time or higher reductant levels. Finally, this also demonstrates that the extra regeneration observed with the longer regeneration time is solely due to the extra time for reaction (1) to continue.

Table 3
Calculated amount of NO_X (μmol) trapped and unreduced NO_X released during regeneration at 200 °C with and without reductant in the regeneration portion of the cycle.

Regeneration protocols	NO_X trapped	NO_X released	Difference
4 s–4% H_2	45	7	38
8 s–2% H_2	49	10	39
16 s–1% H_2	57	16	41

Beyond just the amount of nitrate or nitrite species that decompose with time, there are other routes, still a function of the regeneration time, which might contribute to the improved performance with long regeneration times. The release/desorption and re-adsorption of the NO_X species from trapping sites to adjacent or downstream Ba sites during regeneration events is one such possibility. At low operating temperatures, the desorption rate of NO_X is slower than the reduction rate [5]. Therefore, extending the regeneration event could allow more released NO_X to spillover to adjacent Pt sites for reduction, or be re-adsorbed at downstream Ba sites and then eventually reduced to N_2 as the reductant propagates from the front to back portion of the catalyst. Another scenario, along the same concept, but also related to the time effect related to reaction (1) and discussed above, is that NO_X species can be trapped on two types of Ba sites; as proposed in the literature [34–36], one in close proximity to Pt sites, the other more remote from Pt sites. In previous studies [24], it was shown that Pt can catalyze the decomposition of nitrate species during the regeneration event. The nitrate species trapped on “distant” Ba sites can also be released, but at a slower rate than those proximal to Pt sites [5,24]. Therefore, if the regeneration time is prolonged, it could lead to more NO_X release from both Ba site types. With more NO_X release, there are more sites available in the next trapping phase.

Although no differences in catalyst performance would be expected when either H_2 or NH_3 is used as the reductant source [37], the following brief discussion is only to relate the NH_3 formation trends with different regeneration protocols. The NH_3 concentrations as a function of time at 200 °C and for the three different regeneration protocols are shown in Fig. 5. Ammonia formation upon NO_X reduction with H_2 over NSR catalysts has been widely reported [38–40]. Ammonia was consistently observed in our experiments shortly after the onset of the regeneration phase (about 1–2.5 s after the onset) and reached a maximum when the released NO_X concentration decreased to close to the baseline level, as shown in Fig. 5. This result is consistent with NH_3 formed along the catalyst participating in the reduction of NO_X following the selective catalytic reduction (SCR) mechanism. Ammonia formed at the front of the catalyst is used in

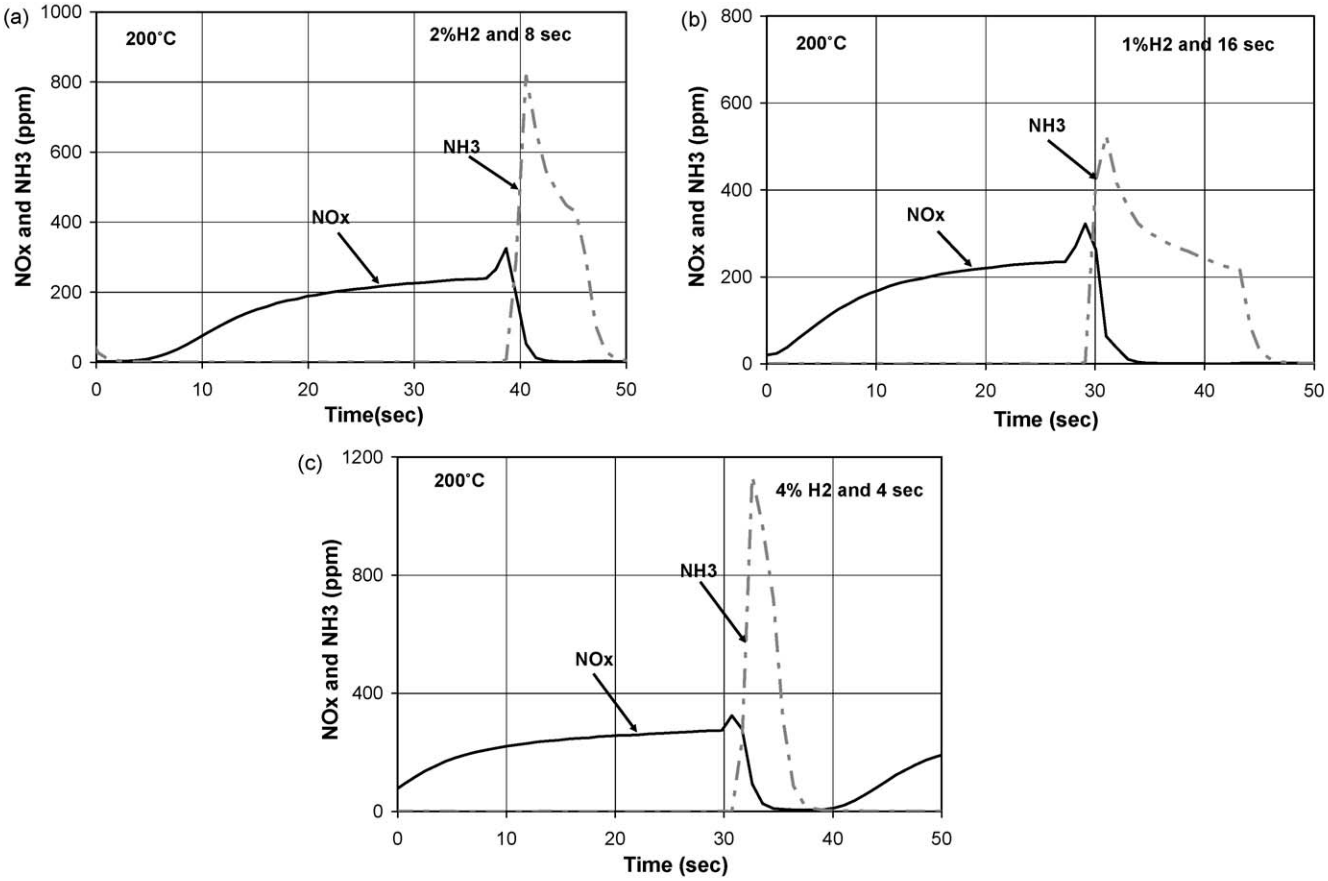

Fig. 5. NH_3 and NO_X outlet concentration data obtained at 200 °C during different regeneration protocols.

the SCR mechanism to reduce downstream nitrate species. As the amounts of nitrates decrease and therefore the amount of NO_X release begins to decrease, less NH_3 formed upstream reacts downstream and more is then observed. The amounts of NH_3 formed during the cycling experiments were calculated as a function of temperature and regeneration time and are listed in Table 2. At 200 and 300 °C, total NH_3 formation was always higher when longer regeneration times were used. However, as shown in Fig. 5, peak NH_3 concentrations were observed with the higher reductant levels, or shorter regeneration times. These trends can be related back to local reductant-to-NO_X ratios, with the higher the ratio leading to more NH_3 formed [41,42], as well as nitrate exposure time to reductant. As shown in Fig. 5, NO_X release occurs at the onset of the regeneration phase. As the regeneration time progresses, less NO_X is being released while reductant is still being delivered, and this results in NH_3 formation accelerating when the observed NO_X release was decreasing. Nitrates were still decomposing, as is evident by the NH_3 formation. Therefore, at later regeneration times, the local reductant-to-NO_X ratio is higher, thus the increase in NH_3 as NO_X decreases. With the shorter regeneration time, but higher reductant level, the increased reductant-to-NO_X ratio led to increased peak NH_3 formation values, while for the longer regeneration time experiments, the longer time led to a larger integral amount of NH_3 formed. At 400 °C, there was not a significant change in the amount of NH_3 formed as a function of regeneration time, likely due to a balance in the more rapid release and reductant-to-NO_X ratio. At 200 and 300 °C, the reductant-to-NO_X ratio was relatively higher due to the higher thermal stability of nitrate species. Therefore, more NH_3 was formed with longer regeneration time due to the increased total amount of NO_X release. However, at 500 °C, the weak stability of nitrate species, and the higher reductant concentration during the shorter regeneration protocol, resulted in higher NH_3 formation since both reactants for NH_3 formation were present in abundant quantities. Overall, at low operating temperatures, the longer regeneration time is a key factor controlling the total release of trapped NO_X and to some extent the formation of NH_3 while at higher operating temperatures, where the thermal stability of nitrate species is weak, the higher reductant concentration is the more important parameter for NH_3 formation.

4. Conclusions

In this study, the effects of three different regeneration protocols between 200 and 500 °C were investigated over a model NSR catalyst. The regeneration conditions were 4, 8 and 16 s with 4, 2, and 1% H_2 as the reductant amounts, respectively. The data showed an obvious improvement in the catalyst performance with increasing regeneration time at 200, 300 and 400 °C, with the effect related to improved NO_X trapping. At 500 °C, the weaker stability of nitrate species resulted in an overall lower conversion due to a more significant amount of NO_X released with decreasing reductant concentrations, although the trapping performance was still better with longer regeneration time. The improved trapping performance with longer regeneration times was primarily due to prolonged regeneration conditions leading to more extensive nitrate decomposition, allowing more NO_X to be trapped in the subsequent trapping phase. Total NH_3 formation at 200 and 300 °C was also higher with longer regeneration time, while at 500 °C, the trend was reversed, and was related to the local reductant-to-NO_X ratios.

Acknowledgements

The authors would like to thank Natural Sciences and Engineering Research Council of Canada Discovery Grant Program and Kuwait University for financial support and Johnson Matthey for the sample provided.

References

[1] M. Bogner, B. Kramer, S. Krutzsch, D. Pischinger, G. Voigtlander, F. Wenninger, M. Wirbeleit, R. Brogan, D. Brisley, Webster, Applied Catalysis B: Environmental 7 (1995) 153.
[2] N. Miyoshi, S. Matsumoto, K. Katoh, T. Tanaka, J. Harada, N. Takahashi, K. Yokota, M. Sugiura, K. Kasahara, SAE Technical Paper Series 950809.
[3] S. Matsumoto, Catalysis Today 29 (1996) 43.
[4] N. Takahashi, H. Shinjoh, T. Iijima, T. Suzuki, K. Yamazaki, K. Yokota, H. Suzuki, N. Miyoshi, S. Matsumoto, T. Tanizawa, T. Tanaka, S. Tateishi, K. Kasahara, Catalysis Today 27 (1996) 63.
[5] W.S. Epling, L.E. Campbell, A. Yezerets, N.W. Currier, J.E. Parks, Catalysis Reviews 46 (2004) 163.
[6] B. Westerberg, E. Fridell, Journal of Molecular Catalysis A: Chemical 165 (2001) 249.
[7] J. Kwak, D. Kim, T. Szailer, C.H.F. Peden, J. Szanyi, Catalysis Letters 111 (2006) 3.
[8] S. Poulston, R.R. Rajaram, Catalysis Today 81 (2003) 603.
[9] D. James, E. Fourré, M. Ishii, M. Bowker, Applied Catalysis B: Environmental 45 (2003) 147.
[10] P. Jozsa, E. Jobson, M. Larsson, Topics in Catalysis 30/31 (2004) 177.
[11] H. Abdulhamid, E. Fridell, M. Skoglundh, Topics in Catalysis 30/31 (2004) 161.
[12] T. Lesage, C. Verrier, P. Bazin, J. Saussey, M. Daturi, Physical Chemistry Chemical Physics 5 (2003) 4435.
[13] Z. Liu, J.A. Anderson, Journal of Catalysis 224 (2004) 18.
[14] M. AL-Harbi, W.S. Epling, Applied Catalysis B: Environmental 89 (2009) 315.
[15] Y. Li, S. Roth, J. Dettling, T. Beutel, Topics in Catalysis 16/17 (2001) 1.
[16] J.P. Breen, C. Rioche, R. Burch, C. Hardacre, F.C. Meunier, Applied Catalysis B: Environmental 72 (2007) 178.
[17] W.S. Epling, A. Yezerets, N.W. Currier, Catalysis Letters 110 (2006) 143.
[18] I. Nova, L. Lietti, L. Castoldi, E. Tronconi, P. Forzatti, Journal of Catalysis 239 (2006) 244.
[19] A. Amberntsson, H. Persson, P. Engstrom, B. Kasemo, Applied Catalysis B: Environmental 31 (2001) 27.
[20] T.J. Toops, D.B. Smith, W.S. Epling, J.E. Parks, W.P. Partridge, Applied Catalysis B: Environmental 58 (2005) 255.
[21] W.S. Epling, L.E. Campbell, J.E. Parks, Catalysis Letters 90 (2003) 45.
[22] S. Hodjati, K. Vaezzadeh, C. Petit, V. Pitchon, A. Kiennemann, Catalysis Today 59 (2000) 323.
[23] P. Schmitz, R. Baird, Journal of Physical Chemistry B 106 (2002) 4172.
[24] J.M. Coronado, J.A. Anderson, Journal of Molecular Catalysis A: Chemical 138 (1999) 83.
[25] J. Despres, M. Koebel, O. Krocher, M. Elsener, A. Wokaun, Applied Catalysis B: Environmental 43 (2003) 389.
[26] H. Fang, J. Wang, R. Yu, C. Wan, K. Howden, SAE Technical Paper Series 2002-01-2889.
[27] L. Olsson, B. Westerberg, H. Persson, E. Fridell, M. Skoglundh, B. Andersson, Journal of Physical Chemistry B 103 (1999) 10433.
[28] S. Erkfeldt, E. Jobson, M. Larsson, Topics in Catalysis 16–17 (2001) 127.
[29] W.S. Epling, D. Kisinger, C. Everest, Catalysis Today 136 (2008) 156.
[30] L. Lietti, P. Forzatti, I. Nova, E. Tronconi, Journal of Catalysis 204 (2001) 175.
[31] S. Hodjati, P. Bernhardt, C. Petit, V. Pitchon, A. Kiennemann, Applied Catalysis B: Environmental 19 (1998) 209.
[32] N.W. Cant, M.J. Patterson, Catalysis Today 73 (2002) 271.
[33] F. Rodrigues, L. Juste, C. Potvin, J.F. Tempère, G. Blanchard, G. Djéga-Mariadassou, Catalysis Letters 72 (2001) 59.
[34] W.S. Epling, J.E. Parks, G.C. Campbell, A. Yezerets, N.W. Currier, L. Campbell, Catalysis Today 96 (2004) 21.
[35] M. Piacentini, M. Maciejewski, A. Baiker, Applied Catalysis B: Environmental 60 (2005) 265.
[36] V. Medhekar, V. Balakotaiah, M. Harold, Catalysis Today 121 (2007) 226.
[37] L. Cumaranatunge, S.S. Mulla, A. Yezerets, N.W. Currier, W.N. Delgass, F.H. Ribeiro, Journal of Catalysis 246 (2007) 29.
[38] A. Lindholm, N.W. Currier, E. Fridell, A. Yezerets, L. Olsson, Applied Catalysis B: Environmental 75 (2007) 78.
[39] L. Castoldi, I. Nova, L. Lietti, P. Forzatti, Catalysis Today 96 (2004) 43.
[40] T. Lesage, C. Verrier, P. Bazin, J. Saussey, S. Malo, C. Hedouin, G. Blanchard, M. Daturi, Topics in Catalysis 30/31 (2004) 31.
[41] J.A. Pihl, J.E. Parks, C.S. Daw, T.W. Root, SAE Technical Paper Series 2006-01-3441.
[42] M. AL-Harbi, W.S. Epling, Catalysis Letters 130 (2009) 121.